Progress In Electromagnetics Research C, Vol. 128, 183–193, 2023

A Low Profile Wearable Slot Antenna with Partial Ground for 5 GHz WLAN/WBAN Applications

Nageswara Rao Regulagadda[1, *] and Uppalapati V. R. Kumari[2]

Abstract—This paper presents a low-profile, flexible, and wearable slot antenna for on-body communication. The proposed antenna is designed on a thin polyamide substrate of 0.25 mm height, which is flexible, elastic, and robust in nature. A rectangular patch with different slots acts as the main radiator, and partial ground acts as the bottom conducting plane for the proposed antenna. The designed antenna was able to resonate in the desired frequency band with a good return loss (S_{11}) by modifying the size of the ground plane along its width and placing a small cut on the ground. The designed antenna achieved a good -10 dB impedance bandwidth of 710 MHz and a peak gain of 7.2 dBi at 5 GHz. The designed antenna was checked for detuning in a bending scenario. The specific absorption rate (SAR) was evaluated, and the values were found to be within standard limits. The designed antenna was fabricated and tested in this study. The results showed good agreement between the simulated and measured values of the antenna parameters. The small size, low weight, and flexibility of the proposed antenna make it a good candidate for wearable devices in the Wireless Local Area Network (WLAN)/Wireless Body Area Network (WBAN) environment.

1. INTRODUCTION

Wearable technologies are making things simpler, more dependable, portable, and inexpensive, and they may be used for health monitoring, wellness, fitness, sports, and military. In a wearable environment, the antenna plays a major role in making the wireless communication link reliable and efficient. Unlike traditional antennas, wearable antennas are hard to design because they have to work very close to human tissue. Since human tissue absorbs electromagnetic energy, this causes the resonant frequency to change. As different parts of the human body have different dimensions and curvatures, the designed antenna should be bent to make it conformable to the human body parts. Even in this bending scenario, the antenna parameters should not be altered much to make it robust. In addition, the design of wearable antennas has constraints like low profile, flexibility, robustness, miniaturization, and low SAR. The design of the wearable antenna while meeting these many constraints is always a challenging task, and a proper selection of substrate material will solve this problem to some extent. So, proper care must be taken by the designer while designing wearable antennas. For antenna designs, microstrip patch antennas are preferable as they are planar structures and offer small size, low cost, and light weight, and they can be easily integrated into microwave integrated circuits [1, 2]. Patch antennas are useful for designing wearable, but their limited bandwidth, poor radiation qualities, low gain, cross polarization, and surface wave production (depending on the feeding environment) make them impractical [3]. To achieve good performance characteristics for microstrip patch antennas, several methods like Energy Band Gap [4], Artificial Magnetic Conductor [5], and Partial Ground [6] are used. Some miniaturization techniques like Frequency Selective Surfaces [7], Defected Ground Structure [8], and Metasurface [9] are

Received 4 December 2022, Accepted 29 December 2022, Scheduled 11 January 2023
* Corresponding author: Nageswara Rao Regulagadda (nageswararao.regula@gmail.com).
[1] Department of ECE, University College of Engineering JNTU Kakinada, East Godavari, India. [2] University College of Engineering JNTU Kakinada, East Godavari, India.

also reported. Using different shapes of slots for increasing impedance bandwidth [6–14], using arrays for gain improvement, using slits, vias, shorting pins, and some other methods were developed. The losses with microstrip line feeding can be improved by going for different feeding methods like coplanar waveguide (CPW), grounded CPW, inset feeding, and Substrate Integrated Waveguide technology.

In this work, rectangular and triangular slots are etched out from the patch to change the electrical path of current on the patch, and the concept of partial ground is used to obtain better performance for the proposed antenna.

2. ANTENNA DESIGN

For the design of proposed antenna, a flexible polyamide fabric is used as a substrate, which is a strong, elastic, lightweight, and durable synthetic material and has electrical properties like a dielectric constant of 4.3, a loss tangent of 0.004, and a thickness of 0.25 mm.

To excite the proposed antenna, a 50 Ω transmission line is used. Firstly, a rectangular patch is chosen as per the conventional microstrip patch antenna dimensions mentioned in [13] as a primary radiator with a full ground plane, but it is not resonated. After that the full ground plane is reduced to partial ground, and the dimensions of the patch are optimized to get the resonance for the proposed antenna. On the patch, initially, a cross-shaped slot is placed to improve the return loss, and then four triangle-shaped slots are placed in the four quadrants formed by the cross-shaped slot in view of improvement in the antenna parameters. Finally, a small cut is placed on the ground to reduce the return loss further and to improve the S_{11} parameter which leads to the desired antenna design. The proposed antenna has a small size of $16.5 \times 16.5 \times 0.25\,\text{mm}^3$ with a radiating patch of size $14.5 \times 9.75\,\text{mm}^2$ as the top layer and a partial ground of size $16.5 \times 1.5\,\text{mm}^2$ as the bottom layer as depicted in Figure 1, and the prototype is depicted in Figure 2. The optimized dimensions of the proposed antenna are illustrated in Table 1.

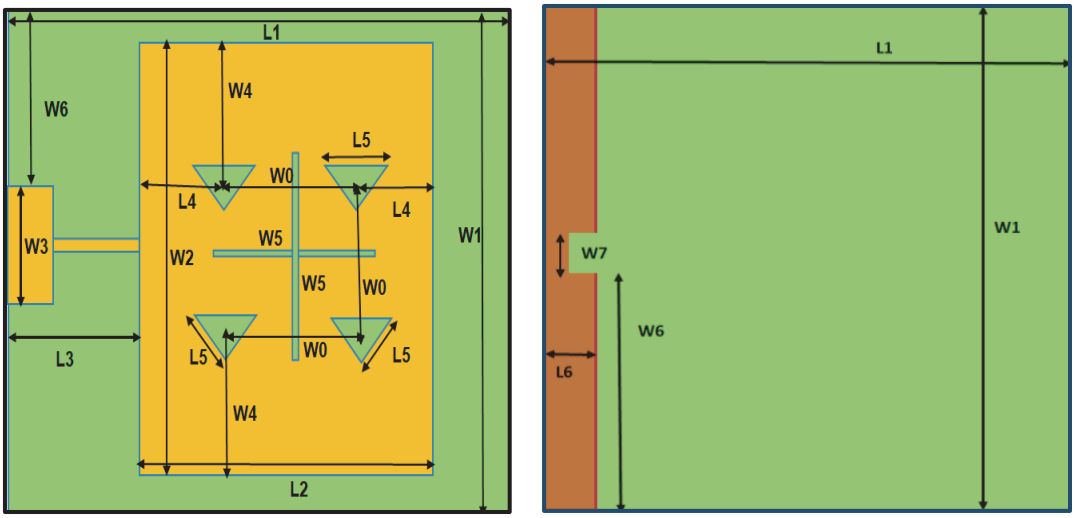

(a) (b)

Figure 1. Proposed antenna design. (a) Top view. (b) Bottom view.

Table 1. Antenna dimensions of the proposed antenna.

Dimension	$W0$	$W1$	$W2$	$W3$	$W4$	$W5$	$W6$	$W7$	$L1$	$L2$	$L3$	$L4$	$L5$	$L6$
Value (mm)	4.5	16.5	14.5	3	4	7	8.15	0.75	16.5	9.75	4	3	2	1.5

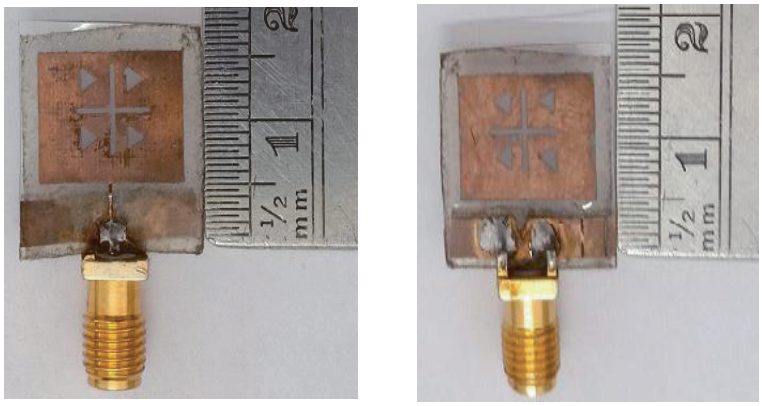

(a) (b)

Figure 2. Proposed antenna prototype. (a) Top view. (b) Bottom view.

3. PARAMETRIC ANALYSIS OF PROPOSED ANTENNA

The obtained results are displayed in Figure 3. Figure 3 shows the simulated results for the evolution of the proposed design in terms of return loss at the desired frequency. Initially, a rectangular patch is chosen with a full ground plane, but the antenna is not resonated, and to get it resonated, the ground is adjusted. The ground plane is minimized until the antenna is resonated, and now the ground plane is simply an I-shaped stub placed along the full width of the patch and 1.75 mm wide along the length of the patch. After that, a slot of cross-shape is placed on the patch, which slightly shifts the frequency band towards lower frequencies, and return losses are degraded. Then, four triangle-shaped slots are placed in the four quadrants formed by the cross-shaped slot, which shifts the resonating frequency slightly towards the higher frequencies, and a small improvement in return loss is achieved. Finally, a cut in the middle of the partial ground results in a significant improvement in the return loss (S_{11}), as illustrated in Figure 3(a). The proposed antenna is resonated at a center frequency of 4.9867 GHz with a good amount of return loss (−43 dB) and has an impedance bandwidth (−10 dB) of 470 MHz (4.8–5.23 GHz). Initially, the antenna is resonated at 4.9866 GHz with an S_{11} value of −24 dB and a bandwidth of (4.79–5.2 GHz), and then a cross shaped slot is placed on the patch to change its behavior, resonated at 4.96 GHz (4.76–5.18 GHz). Then, four triangular slots are placed on the patch to improve antenna performance further, resonated at 4.9977 GHz (4.79–5.18 GHz) with S_{11} value of −23 dB, and then a small portion of the ground is cut, resulting in the proposed antenna.

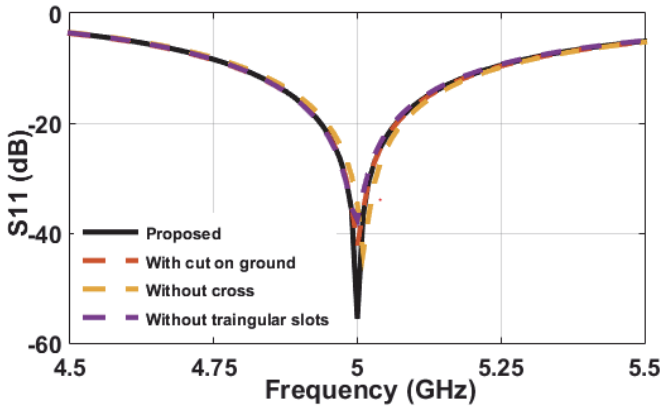

Figure 3. S_{11} plot of proposed antenna for varying ground and patch structures.

The proposed antenna is analyzed for variation in return loss value (S_{11}) with variations in different parts of the antenna like placement of feed point at different lengths from the origin in positive X-direction ($W6$), length of the patch ($L2$), different lengths of the ground ($L6$), as depicted in Figure 4. Figure 4(a) illustrates the results for placing the proposed antenna at different distances from the origin in the positive X-direction. This parameter is evaluated for 8.75 mm (proposed), 9 mm (shifts the resonating frequency towards higher frequencies and increases the return losses), 10 mm (it resonates at nearly 5 GHz but increases return losses), 10.5 mm (shifts the resonating frequency towards lower frequencies and increases the return losses), and beyond 11 mm and below 8.5 mm result in degraded performance for the proposed antenna.

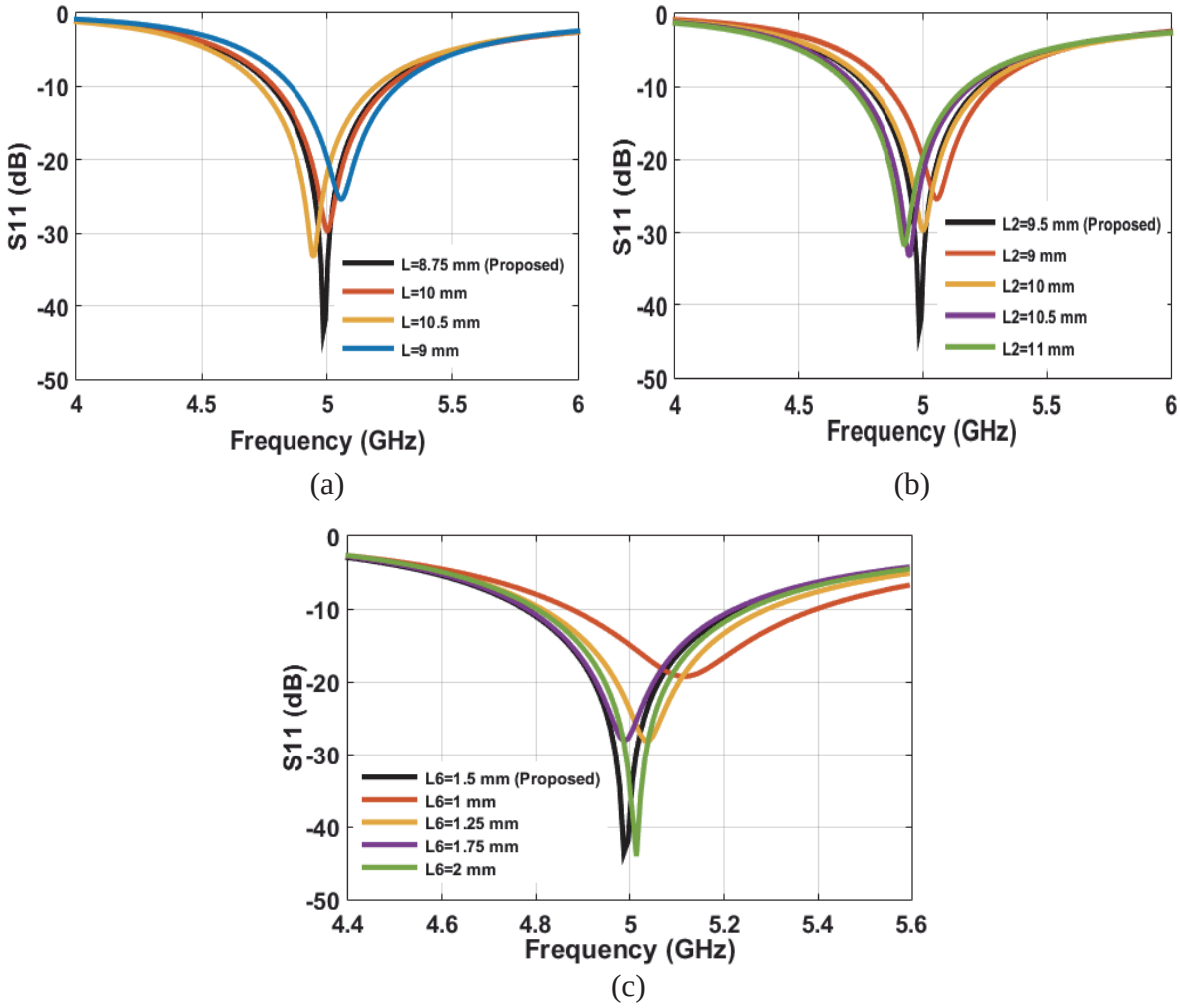

Figure 4. S_{11} plot of proposed antenna for (a) Different positions of the feed point from the origin in positive X-direction ($W6$), (b) Different lengths for the patch ($L2$), (c) Different lengths of the ground ($L6$).

Figure 4(b) depicts the change in return loss (dB) for different lengths of $L2$ (mm). The proposed value of $L2$ is 9.5 mm and for $L2$ is 9 mm. The resonating frequency shifts towards high frequencies with a return loss of -24 dB; for 10 mm, the resonating frequency shifts towards desired frequency with a small improvement in return losses; a further increase in the value of $L2$ is 10.5 mm, and the resonating frequency shifts towards lower frequencies with a return loss of -32 dB. Further increment in $L2$ value results in detuning and performance degradation in terms of return loss or reflection coefficient. The shift in resonating frequency towards higher frequencies is due to the change in inductance offered by the dimensions of the patch. Figure 4(c) illustrates the change in return loss (dB) for L6 with different

values. The proposed value of $L6$ is 1.5 mm and for L6 is 1 mm, and the resonating frequency shifts towards high frequencies (5.518 GHz) with a return loss of more than −20 dB. With $L6$ at 1.25 mm, the resonating frequency shifts towards the desired frequency with a return loss of −30 dB. With a further increase in the value of $L6$ to 1.75 mm, the resonating frequency shifts towards the proposed value with a return loss of −30 dB. A further increment in $L6$ value to 2 mm results in the desired antenna parameter values. These changes are due to the change in reactance offered by the ground plane.

4. SIMULATION AND MEASURED RESULTS

For the designed antenna, the simulation was done with the EM Full-Wave simulator HFSS and tested using VNA (Vector Network Analyser) — Keysight FieldFox Microwave Analyzer N9917A. After the verification of simulated results, fabrication is done for the proposed antenna, and it is tested using network analyzers.

The measured values of antenna parameters are depicted in Figure 5. The measured results show an impedance bandwidth of 710 MHz over a span of 4.68–5.39 GHz, fractional bandwidth of 14%, a peak S_{11} of −28 dB, and the measured value of the gain is about 7.2 dB at center frequency (5.05 GHz). The measured bandwidth is improved from 470 MHz to 710 MHz, and the gain is decreased from 7.7 dBi to 7.2 dBi, compared with the simulated results. The difference in simulated and measured results may be due to the simulator tool's inefficiency. Figure 5(a) shows the measured return loss, S_{11}, and Figure 5(b) depicts the measured gain in dB. Figure 5(c) depicts the measured radiation patterns in E-plane and H-plane, and Figure 5(d) represents the prototype of the proposed antenna in an anechoic chamber for pattern measurement.

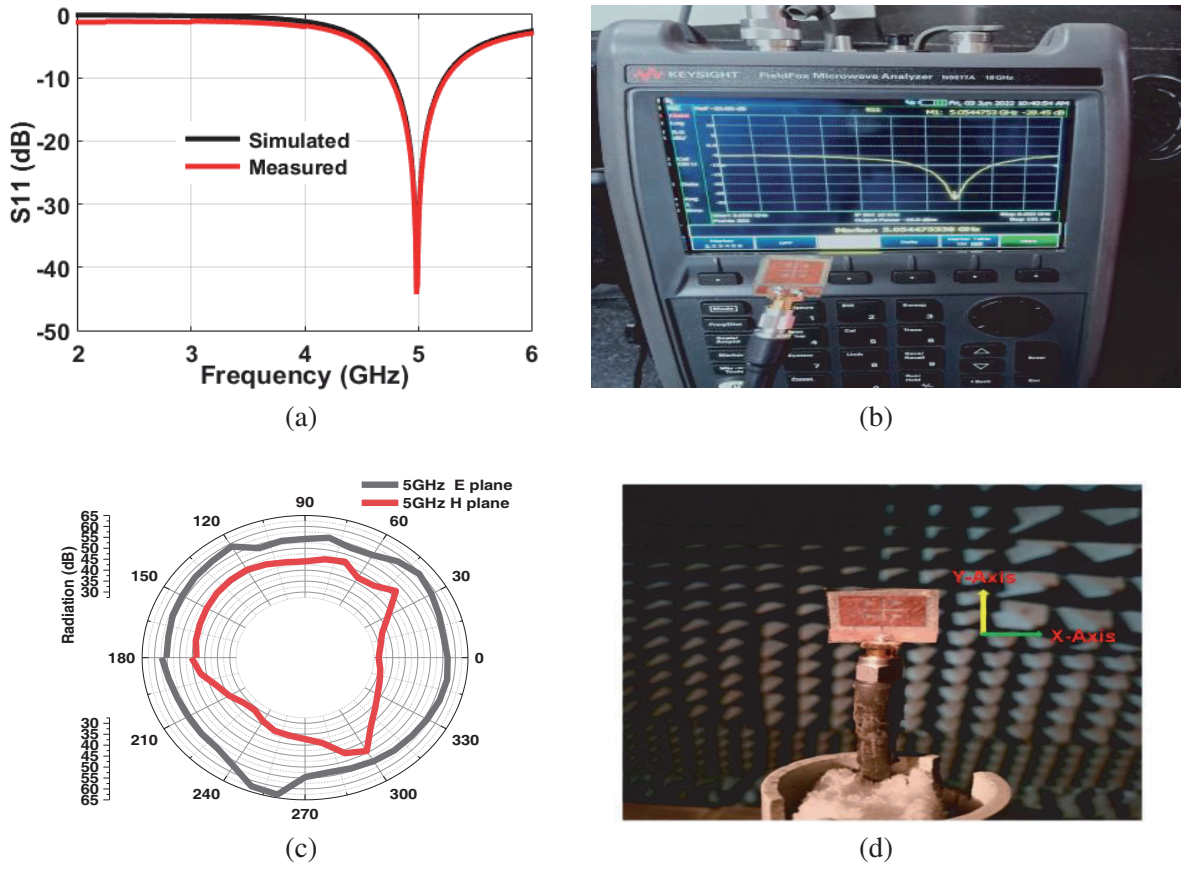

Figure 5. Proposed antenna. (a) Simulated and measured return loss, S_{11}. (b) Photograph of measured S_{11}. (c) Radiation Pattern of fabricated antenna in both E-Plane and H-Plane. (d) Proposed antenna in Anechoic chamber.

4.1. Wearability Test

The proposed antenna is designed for wearable environment. In order to test this antenna's wearability, it is analyzed for its stability in bending conditions, effect of human loading on it, and its SAR value, and this analysis is done in the following sections.

4.1.1. Bending Analysis

In an on-body scenario, in a wireless body area network environment (WBAN), or especially in a wearable environment, the designed antenna should be conformal to that of the different shapes of different body parts of a human. For that, the designed antenna has to be analyzed for the change in its parameter values in bending scenarios.

The bending of the proposed antenna is done both in X and Y directions with radii of 10 mm, 20 mm, and 30 mm, and its effects are analyzed in terms of detuning of the resonating frequency. Figure 6(a) shows the bending structure of the proposed antenna in the X direction, and the respective analysis is depicted in Figure 6(b). Figure 6(c) and Figure 6(d) show the antenna bending structure and its analysis in the Y direction, respectively. The variations in antenna parameters like resonating frequency, return loss, bandwidth, and gain values in bending analysis are explained in Table 2.

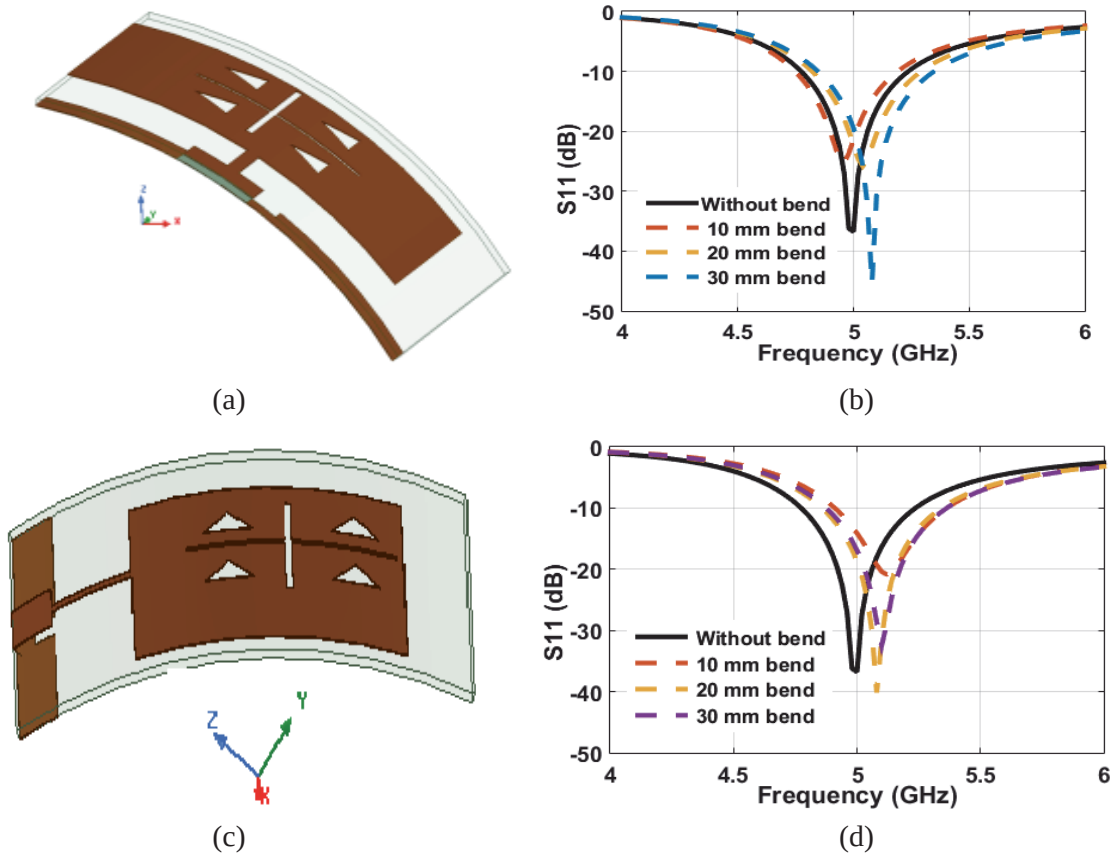

Figure 6. Bending Scenario. (a), (b) Proposed antenna is bent in X-direction with its effect on resonating frequency. (c), (d) Proposed antenna is bent in Y-direction with its effect on resonating frequency.

4.1.2. Human Loading

To analyze the variations in antenna parameter values when the antenna is placed near the human tissues, a 3-layer human tissue model is prepared using an HFSS simulator. The three layers in the

Table 2. Parameter variations of proposed antenna in bending scenario.

Bending	Frequency (GHz)	S_{11} (dB)	Bandwidth (MHz)
X-bent (10 mm)	5.04	−25	4.82–5.29
X-bent (20 mm)	4.96	−25	4.75–5.19
X-bent (30 mm)	5.08	−45	4.85–5.35
Y-bent (10 mm)	5.12	−21	4.91–5.36
Y-bent (20 mm)	5.08	−40	4.86–5.34
Y-bent (30 mm)	5.10	−32	4.88–5.36

human tissue model are skin, fat, and muscle, respectively, from top to bottom. The electrical properties such as relative permittivity, conductivity, and dielectric loss tangent of these three layers are taken from [9] and are depicted in Table 3, and the respective human tissue model is shown in Figure 7. From Figure 7, it is clear that the antenna bottom plane (ground) is placed on the skin tissue of 2 mm in height, which is the upper layer of the human tissue model. The skin layer is followed by a fat layer of 5 mm in height, and the fat layer is followed by a muscle layer of 20 mm, chosen for the analysis of the proposed antenna.

The change in antenna parameter values has been studied and is presented in Figure 8. Firstly, the proposed antenna was placed on the human tissue and found to resonate at 4.82 GHz with a return

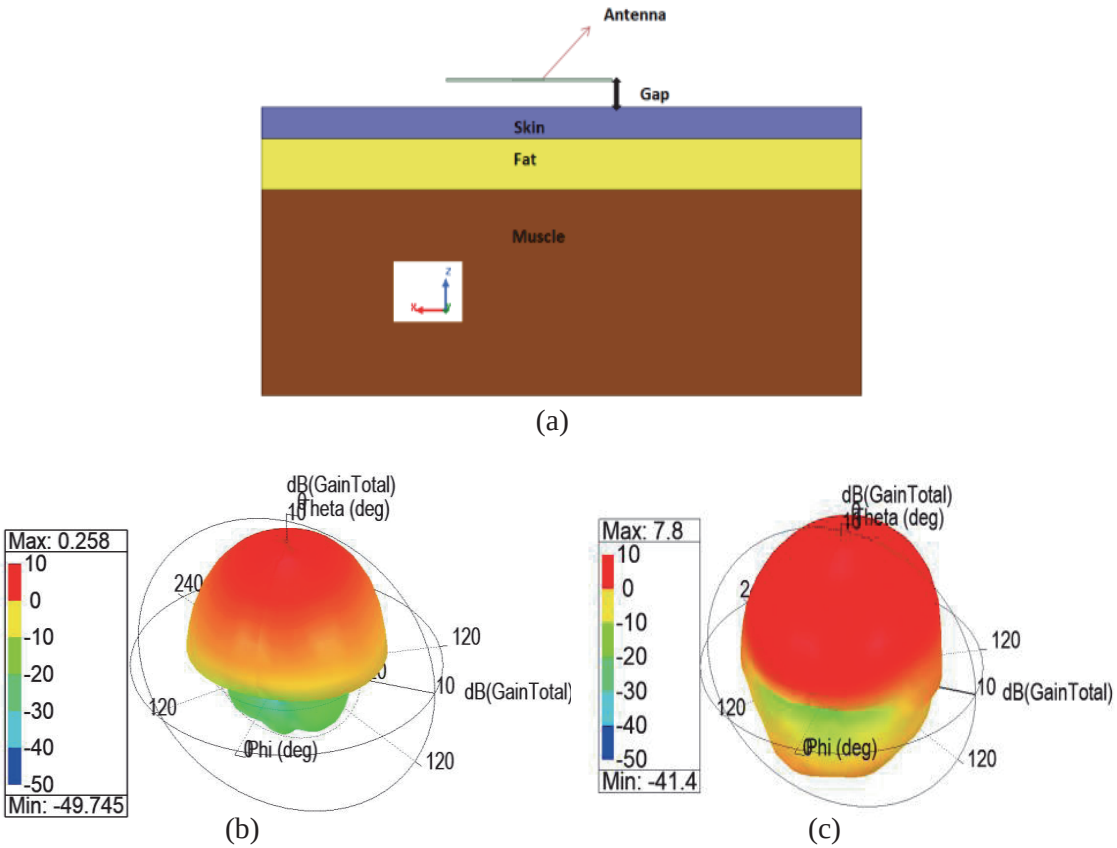

Figure 7. Proposed antenna. (a) Three layer human tissue model used in the analysis of effects of human loading on the antenna parameters. (b) Gain polar plot when antenna is placed on human tissue model with a gap of 5 mm. (c) Gain plot when antenna is placed on human tissue model with a gap of 5 mm.

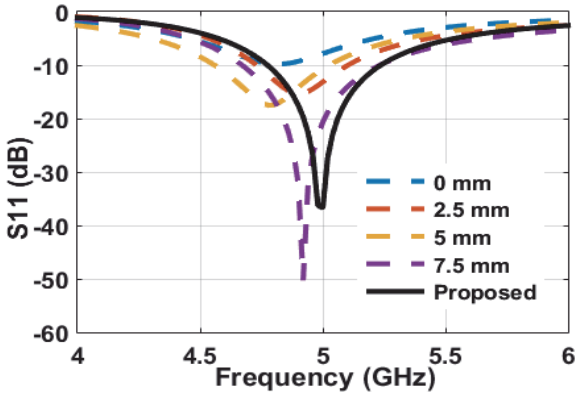

Figure 8. Antenna detuning when it is loaded with human tissues.

loss of −9 dB and a negative gain. Thus, the proposed antenna is not meeting desired values of antenna parameters like a good amount of −10 dB bandwidth, a small amount of positive gain, and low detuning in resonating frequency. Then the analysis is done by maintaining some gap between the antenna of interest and the human tissue. The gap value is varied from 0 mm to 7.5 mm in increments of 2.5 mm, and the respective values of S_{11} and gain for each case are presented in Table 4. The deviation in antenna parameter values may be due to the change in dimensions of the antenna when it is bent. Because when the antenna is rolled over a cervical structure, the dimension of the top portion of a layer does not match that of the bottom portion. Based on the findings, it is clear that placing an antenna directly on human tissue with a gap greater than 5 mm is not recommended for practical applications, and a minimum gap of 2.5 mm should be maintained between the proposed antenna and the human tissue. The proposed antenna gain plots are depicted in Figures 7(b) and (c).

Table 3. Electrical properties of Human Tissues.

Human Tissues	**Relative Permittivity (ε_r)**	**Conductivity (s/m)**	**Loss Tangent (tan δ)**	**Density (kg/m^3)**
Skin	35.11	3.72	0.3076	1100
Fat	4.95	0.29	0.17315	910
Muscle	48.48	4.96	0.29353	1041

Table 4. Effect of Human Loading on the proposed antenna parameter values.

Gap (mm)	Res. Freq. (GHz)	S_{11} (dB)	Gain (dB)
0 mm	4.82	−17.28	0.258
2.5 mm	4.78	−15.39	5.4
5 mm	4.92	−17.98	5.8
7.5 mm	4.92	−51.86	7.8

4.1.3. SAR Calculation

The parameter, Specific Absorption Rate (SAR), is used to determine the effect of electromagnetic exposure on the human body. The SAR is a vital parameter for human wellness in the wearable environment. The designed antenna should fall below standards set for the SAR level of 1.6 W/ kg per

1 g tissue as per US (United States) standard and below 2 W/kg per 10 g tissue as per EU (European Union) standard. The theoretical calculation of SAR is presented as follows:

$$SAR = \sigma E^2/\rho \tag{1}$$

where $'\sigma'$ is the conductivity of human tissue, 'E' the electric field intensity, and 'ρ' the mass density human tissue.

The average SAR of the proposed antenna is analyzed on a 3-layer human tissue model whose properties are mentioned in Table 4, and the obtained average SAR value of the proposed antenna for without a cut on the ground and with a cut on the ground is depicted in Figures 9(a) and 9(b), respectively. It is evident from the obtained simulated results that the proposed antenna without a cut on the ground does not fall within the standards of SAR value, and the antenna with a cut on the ground and with a low input power of less than 500 mW falls within the standards set for SAR value. In

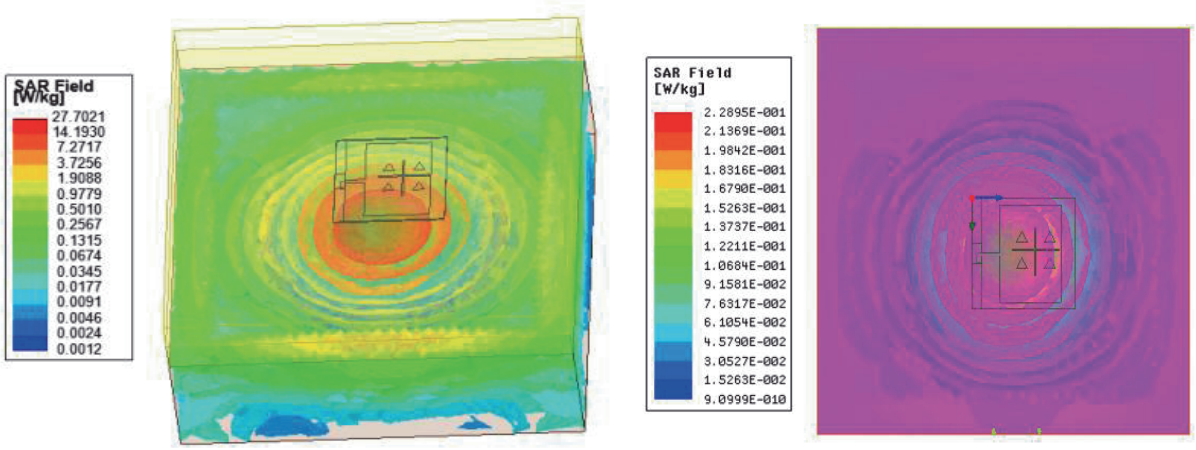

Figure 9. SAR Calculation, (a) without cut on the ground, (b) with cut on the ground and with low input power.

Table 5. Comparison of proposed work with the literature.

Reference	Antenna dimensions (mm^3)	Dielectric material	Type of miniaturization	Frequency (GHz)	Bandwidth (GHz)	Gain dBi	SAR W/kg
[5]	102 × 68 × 3.6	Textile	AMC	5.8	4.30–5.9	6.12	0.37
[7]	28 × 28 × 3	Acrylic fiber	FSS with DGS	5.51	5.41–5.60	2.9	NA
[9]	42 × 28 × 4	Textile	Metasurface	5	4.96–5.9	6.7	1.06
[11]	30 × 30 × 0.787	Rogers RT5880	Rectangular slot	5.8	0.45	2.75	20
[13]	60 × 60 × 3	PDMS	Rectangular	2.45	2.38–2.52	4.1	0.809
[15]	45 × 35 × 2.5	Wool felt	PIFA	5	5.15–5.825	5.9	0.612
[16]	50 × 50 × 0.7	Dielectric threads	Short circuited patch	5.9	5.65–6.2	2.75	NA
[17]	60 × 20 × 3.2	Textile	HMSIC	5	4.7–5.2	7.2	NA
Proposed	**16.5 × 16.5 × 0.25**	**Polyamide**	**Triangular & rectangular**	**5**	**4.68–5.39**	**7.2**	**0.228**

order to minimize SAR value, the input power of the device operating near the human body is limited to 295 mW. These limitations on the input power are reported in [18]. In some cases [19], polymeric ferrite shielding is used to reduce SAR values as the ferrites are found to be effective in diminishing electromagnetic influence.

In comparison to [5, 7, 9, 11, 13, 15–17], the proposed antenna is small in size, with a low profile and good gain, and the substrate thickness is low (0.25 mm), making it suitable for on-body use. It is a simple design having slots on the patch with partial ground as that of all other designs like AMC (Artificial Magnetic Conductor), EBG (Electromagnetic Band Gap Structure), PIFA (Planar Inverted-F Antenna), Fractals, Meta surfaces, and SIW (Substrate Integrated Waveguide) technology presented in Table 5.

5. CONCLUSIONS

The proposed antenna is designed on a flexible polyamide substrate of 0.25 mm, and the size of the antenna is 16.5 mm × 16.5 mm to make it suitable for wearable environments at 5 GHz. The desired frequency band with good return-loss was achieved with the use of partial ground, by altering the dimensions of the ground plane and by cutting a small portion out of the ground. The designed antenna was fabricated and tested. The fabricated antenna achieved a good impedance bandwidth of 710 MHz and a high gain of more than 7.2 dB at a center frequency of 5.05 GHz. The designed antenna was checked for detuning in bending scenario, both in X and Y directions, and SAR was also evaluated with and without a cut on the ground. The simulated SAR value of the proposed antenna with an input power of less than 500 mW is 0.22 watts per kg, which is far below the limit of the US standard that is 1.6 W (watts) per kg (kilogram) per 1 g of tissue. The results showed good agreement between the simulated and measured values of antenna parameters. The small size, low weight, and flexibleness of this antenna satisfy the requirements of wearable applications, and its omnidirectional radiation pattern makes this antenna a valid candidate for on-body communication applications in WBAN/WLAN environment.

REFERENCES

1. Devana, V. N., V. Satyanarayana, A. Vijaya Lakshmi, Y. Sukanya, Ch. Kumar, V. L. N. Ponnapalli, and K. J. Babu, "A novel compact fractal UWB antenna with dual band notched characteristics," *Analog Integrated Circuits and Signal Processing*, Vol. 110, 349–360, 2022.
2. Koteswara Rao Devana, V. N. and A. Maheswara Rao, "A compact fractal dual high frequency band notched UWB antenna with a novel SC-DGS," *Analog Integrated Circuits and Signal Processing*, Vol. 107, 145–153, 2021.
3. Balanis, C. A., *Antenna Theory: Analysis and Design*, John Wiley and Sons, New York, 2004.
4. Low, J.-H., P.-S. Chee, and E.-H. Lim, "Liquid EBG-backed stretchable slot antenna for human body," *IEEE Transactions on Antennas and Propagation*, Vol. 70, No. 10, 2022.
5. Alemaryeen, A. and S. Noghanian, "On-body low-profile textile antenna with artificial magnetic conductor," *IEEE Transactions on Antennas and Propagation*, Vol. 67, No. 6, 3649–3656, 2019.
6. Koteswara Rao Devana, V. N. and A. Maheswara Rao, "Design and parametric analysis of beveled UWB triple band rejection antenna," *Progress In Electromagnetic Research M*, Vol. 84, 95–106, 2019.
7. Mandal, B., A. Chatterjee, P. Rangaiah, M. D. Perez, and R. Augustine, "A low profile button antenna with back radiation reduced by FSS," *2020 14th European Conference on Antennas and Propagation (EuCAP)*, 1–5, Copenhagen, 2020.
8. Koteswara Rao Devana, V. N., "A novel UWB monopole antenna with defected ground structure," *International Journal of Signal Processing, Image Processing and Pattern Recognition* Vol. 10, No. 1, 89–98, 2017.
9. Gao, G., C. Yang, B. Hu, R. Zhang, and S. Wang, "A wearable PIFA with an all-textile metasurface for 5 GHz WBAN applications," *IEEE Antennas and Wireless Propagation Letters*, Vol. 18, No. 2, 288–292, 2019.

10. Koteswara Rao Devana, V. N., E. K. Kumari, K. S. Chakradhar, P. K. Sharma, D. Rama Devi, C. M. Kumar, V. D. Raj, and D. R. Prasad, "A novel foot-shaped elliptically embedded patch-ultra wide band antenna with quadruple band notch characteristics verified by characteristic mode analysis," *International Journal of Communication Systems*, Vol. 35, No. 15, e5284, 2022.
11. Li, E., X. J. Li, and B.-C. Seet, "A 5.8 GHz slot antenna with parallel slit loading for 5G conformal and wearable applications," *2021 IEEE Microwave Theory and Techniques in Wireless Communications (MTTW)*, 80–85, Riga, Latvia, 2021.
12. Koteswara Rao Devana, V. N. and A. Maheswara Rao, "A compact flower slotted dual band notched ultrawide antenna integrated with Ku band for ultrawideband, medical, direct broadcast service, and fixed satellite service applications," *Microwave and Optical Technology Letters*, Vol. 63, No. 2, 556–563, 2021.
13. Balanis, C. A., *Antenna Theory: Analysis and Design*, Wiley, Hoboken, NJ, USA, 1997.
14. Koteswara Rao Devana, V. N. and A. Maheswara Rao, "A novel compact tri band notched UWB monopole antenna," *Progress In Electromagnetic Research M*, Vol. 91, 123–134, 2020.
15. Gao, G., S. Wang, R. Zhang, C. Yang, and B. Hu, "Flexible EBG backed PIFA based on conductive textile and PDMS for wearable applications," *Microwave and Optical Technology Letters*, Vol. 62, No. 4, 1733–1741, 2020.
16. Alonso-González, L., S. Ver-Hoeye, M. Fernandez Garcia, Y. Álvarez-López, C. Vázquez-Antuña, and F. L. Andrés, "Fully textile-integrated microstrip-fed slot antenna for dedicated short-range communications," *IEEE Transactions on Antennas and Propagation*, Vol. 66, No. 5, 2262–2270, 2018.
17. Kaufmann, T. and C. Fumeaux, "Wearable textile half-mode substrate-integrated cavity antenna using embroidered vias," *IEEE Antennas and Wireless Propagation Letters*, Vol. 12, 805–808, 2013.
18. Zebiri, C., D. Sayad, I. Elfergani, A. Iqbal, W. F. Mshwat, J. Kosha, J. Rodriguez, and R. Abd-Alhameed, "A compact semi-circular and arc shaped slot antenna for heterogeneous RF front-ends," *Electronics*, Vol. 8, No. 10, 1123, 2019.
19. Augustine, R., T. Alves, T. Sarrebourse, B. Poussot, K. T. Mathew, and J. Laheurte, "Polymeric Ferrite sheets for SAR reduction of wearable antennas," *Electronics Letters*, Vol. 46, No. 3, 197–198, 2010.